

## MAGNETISM AND FERROELECTRICITY

# Unidirectional Anisotropy in $(RE-TM)/NiFe$ Film Systems

V. A. Seredkin\*, R. S. Iskhakov\*, V. Yu. Yakovchuk\*, S. V. Stolyar\*\*, and V. G. Myagkov\*

\* Kirensky Institute of Physics, Siberian Division, Russian Academy of Sciences,  
Akademgorodok, Krasnoyarsk, 660036 Russia

\*\* Krasnoyarsk State University, Krasnoyarsk, 660041 Russia

e-mail: sva@iph.krasn.ru

Received August 12, 2002; in final form, October 14, 2002

**Abstract**—The quasi-static magnetic parameters of TbFe/NiFe and DyCo/NiFe bilayer exchange-biased films characterized by unidirectional anisotropy are studied. The characteristic temperatures are determined at which the unidirectional anisotropy disappears due to processes in the magnetically hard layer. The mechanisms responsible for the appearance of unidirectional anisotropy associated with the heterophase property of the magnetically hard layer are analyzed. © 2003 MAIK “Nauka/Interperiodica”.

### 1. INTRODUCTION

The phenomenon of unidirectional anisotropy in ferromagnets, which manifests itself in a shift of the magnetic hysteresis loop along the axis of the fields, was discovered by Meiklejohn and Bean in oxidized cobalt powders [1]. The physical cause of this phenomenon was ascertained at the same time. The cause of the unidirectional anisotropy was shown to be an exchange interaction at the ferromagnet–antiferromagnet interface under the condition of the collinear orientation of magnetizations of the ferrimagnet and one of the antiferromagnet sublattices. This effect was thoroughly studied in NiFe/NiFeMn and NiFe/FeMn film systems in [2–4]. In [5, 6], the  $(RE-TM)/NiFe$  bilayer systems were produced for the first time. Here,  $(RE-TM)$  is DyCo or TbFe, i.e., a ferrimagnet with perpendicular magnetic anisotropy (PMA), and NiFe is a ferromagnet (permalloy) with uniaxial anisotropy and magnetization in the sample plane. These systems, immediately after evaporation (without annealing), are also characterized by unidirectional anisotropy, and the shift in the hysteresis loop of NiFe ( $\Delta H$ ) along the axis of the fields considerably exceeds the values observed in [1–4] (see Fig. 1a).

The following circumstance was surprising. According to the current concepts of the magnetic structure of ferrimagnetic alloys of  $RE-TM$  compensation compositions, the orientations of the effective magnetization vectors in separate layers of  $(RE-TM)/NiFe$  bilayer films we studied are mutually orthogonal and, hence, are exchange-unbiased. Therefore, the features observed in the magnetization reversal curves for the NiFe layer in these bilayer systems cannot be interpreted within the conventional concepts.

In this work, we investigated the static magnetic properties and the temperature dependences of the static magnetic characteristics in DyCo/NiFe and TbFe/NiFe bilayer exchange-biased films with unidi-

rectional anisotropy. The study was undertaken with the aim of elucidating the real magnetic microstructure of the films of  $RE-TM$  ferrimagnetic alloys with compensation compositions. Note that thin ferrimagnetic films of  $RE-TM$  alloys produced in the form of solid solutions over a wide concentration range are characterized

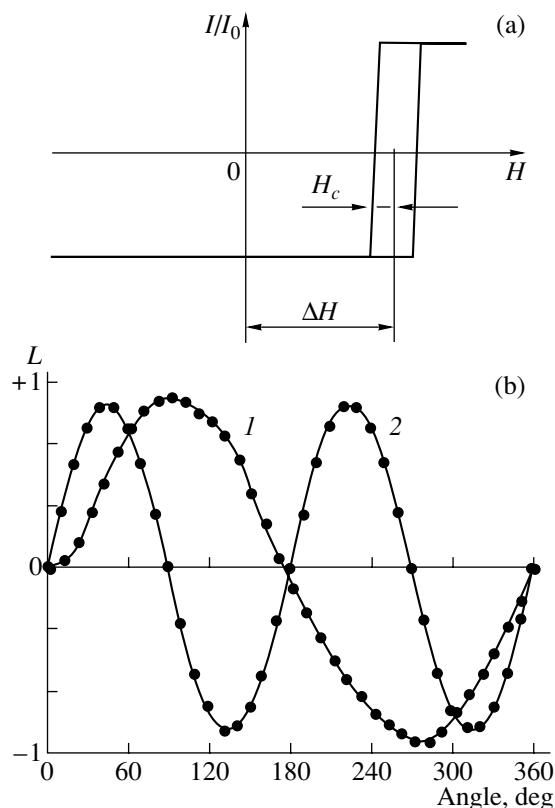


**Fig. 1.** (a) Typical magnetization reversal curve and (b) the angular momentum curves of the (1)  $RE-TM/NiFe$  and (2) NiFe film systems.

Numerical values of the coercive force and the bias field of DyCo/NiFe bilayer films at different thicknesses of NiFe

Thickness, nm	$H_c$ , Oe	$\Delta H$ , Oe
50	4	60
100	2.5	26
150	1.5	14
300	0.7	6
400	0.4	4
700	0.3	2

by the magnetic compensation represented in the concentration–temperature plane by the curve  $x_c(T_{\text{comp}})$ , near which these materials become most magnetically hard. In the vicinity of the compensation temperature  $T_{\text{comp}}$ , these films in general exhibit anomalies: step magnetization curves, anomalous magneto-optic curves, anomalous Hall dependences, etc., which have not yet been properly explained. The necessity of interpreting experimental data requires a search for novel approaches to the study of thin films of *RE–TM* ferrimagnetic alloys. In our opinion, the second layer with known magnetic properties can be used for this purpose. Therefore, the study of the magnetic phenomena in (*RE–TM*)/NiFe bilayer films of (*RE–TM*) compensation compositions is of general physical interest.

## 2. SAMPLES AND EXPERIMENTAL TECHNIQUE

The (*RE–TM*)/NiFe bilayer exchange-biased films were produced through thermal evaporation under a vacuum of  $\sim 3 \times 10^{-6}$  Torr. Cover glasses were used as substrates. The *RE–TM* and NiFe layers were sequentially deposited from three independent evaporators with ring-shaped cathodes. A ferrimagnet (TbFe or DyCo) was represented as a film with a perpendicular magnetic anisotropy of  $\sim 3\text{--}5 \times 10^5$  erg/cm<sup>3</sup> and a coercive force of  $\sim 5\text{--}7$  kOe. According to electron microscopy [7, 8], the ferrimagnetic layer is an amorphous or nanocrystalline alloy with a grain size of  $\sim 5$  nm and the ferromagnetic layer is an NiFe film with uniaxial anisotropy in the sample plane. In order to obtain uniaxial anisotropy in NiFe during evaporation, a dc magnetic field of 20 Oe was applied in the sample plane. The ferrimagnet thickness was  $h = 70$  nm, and the NiFe thickness was varied from 50 to 700 nm. The bilayer samples were produced in the following sequences. (i) The ferrimagnetic layer of precompensation or postcompensation composition was evaporated immediately onto the substrate, and then the NiFe layer was evaporated. (ii) The NiFe layer was evaporated immediately onto the substrate, and then the ferrimagnetic layer was evaporated onto it. We should note that, in case (i), the crystallite size in the NiFe layer is  $\sim 10\text{--}15$  nm, because the amorphism (nanocrystallinity) of a

ferrimagnet (TbFe, DyCo) layer has a significant effect on the formation of the crystal structure of the permalloy layer.

The static magnetic parameters of the magnetization reversal curves and their temperature dependences were measured using a loop scope in fields up to 250 Oe at a frequency of 50 Hz. The angular mechanical momenta were measured at room temperature using a torsional magnetometer in fields up to 12 kOe. In these techniques, a field that reverses the magnetism was applied in the sample plane in the course of the measurements and the ferrimagnetic *RE–TM* layer was always in a saturated state (at room temperature).

An extensive technological search was preliminarily carried out to optimize the growth of the film structures with exchange unidirectional anisotropy. From the application viewpoint, the most acceptable values of the parameters under study were obtained for ferromagnetic films with a nickel content of 80–83%, i.e., for conventional permalloys with zero magnetostriction.

The table lists the magnetic parameters of the DyCo/NiFe bilayer films with exchange unidirectional anisotropy versus the ferromagnetic layer thickness.

## 3. EXPERIMENTAL RESULTS

The dependences of mechanical momenta  $L$  on the angle  $\varphi$  for the DyCo/NiFe bilayer system with unidirectional anisotropy and the NiFe films with uniaxial anisotropy (Fig. 1b) were measured at room temperature using a torsional magnetometer. Similar dependences were also measured for systems with ferrimagnetic TbFe.

The dependence  $L(\varphi)$  measured in the angle range from 0 to 360° can be used to calculate the constants of uniaxial and unidirectional anisotropy ( $K_u$  and  $K_o$ , respectively) by a simple method using the following equations:

$$\frac{L(\varphi) + L(\varphi + \pi)}{2} = K_u \sin 2\varphi, \quad (1)$$

$$\frac{L(\varphi) - L(\varphi + \pi)}{2} = K_o \sin 2(\varphi - \gamma_o), \quad (2)$$

where  $\gamma_o$  is the angle between the easy magnetization axis (EMA) and the direction of unidirectional anisotropy.

The numerical values of  $K_u$  and  $K_o$ , as well as their dependences on the NiFe layer thickness, for the DyCo/NiFe and TbFe/NiFe exchange-biased systems with unidirectional anisotropy are given in Fig. 2.

It can be seen from Fig. 2 that the constants of uniaxial and unidirectional anisotropy of TbFe/NiFe and DyCo/NiFe film systems are characterized by similar dependences on the NiFe film thickness.

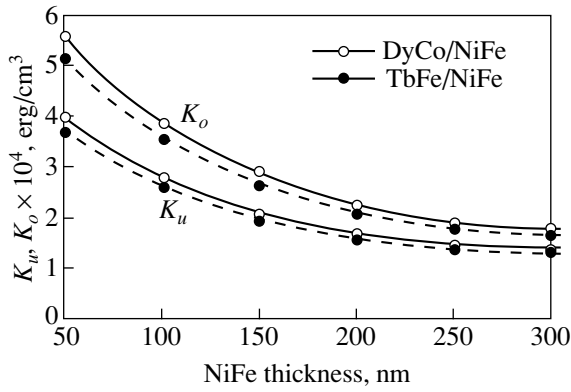


**Fig. 2.** Dependence of the constants of uniaxial ( $K_u$ ) and unidirectional ( $K_o$ ) anisotropies of the (RE-TM)/NiFe film system on the NiFe thickness.

As was noted above, in contrast to [2–4], the bilayer exchange-biased films are characterized by a sharp interface between layers; hence, the specific energy  $E_S$  of the surface interaction should be identical for all the samples and independent of the NiFe layer thickness (while the magnitude of unidirectional anisotropy is inversely proportional to the NiFe layer thickness [9]). We also note that the effective magnetic thickness  $\Delta h_{\text{eff}}$  of the surface exchange interaction between layers (we calculated in [10]) is  $\sim 50$  nm.

The temperature dependences of the coercive force  $H_c$  and the bias fields  $\Delta H$  for (RE-TM)/NiFe bilayer films with unidirectional anisotropy upon magnetization reversal in an ac field were measured at temperatures from +20 to +140°C. The magnetic field was applied along both the EMA and hard magnetization axes (HMA) of the NiFe layer (Figs. 3, 4). It is worth noting that the static magnetic parameters  $H_c$  and  $\Delta H$  change insignificantly in the temperature range from -50 to +60°C, which is important from the application viewpoint.

An analysis of the curves shown in Figs. 3 and 4 demonstrates that there exists a certain temperature ( $\sim 60$  and  $\sim 90^\circ\text{C}$  for TbFe/NiFe and DyCo/NiFe, respectively) at which  $H_c$  and  $\Delta H$  change drastically and the unidirectional anisotropy almost disappears; i.e., the hysteresis loop becomes nearly symmetric with respect to zero field.

Upon magnetization reversal along the HMA, the hysteresis loop of the TbFe/NiFe bilayer film system is not open and is almost symmetric with respect to the zero applied field  $H$ . As the film system is heated from room temperature to  $90^\circ\text{C}$ , the magnetic system does not exhibit any changes. In the range of  $\sim 90^\circ\text{C}$ , the hysteresis loop is sharply opened, which is characterized by the coercive force  $H_c^*$ . In [11], a similar change in the coercive force of DyCo films was observed in the course of their heating and magnetization reversal along the HMA. As compared to the TbFe system, the

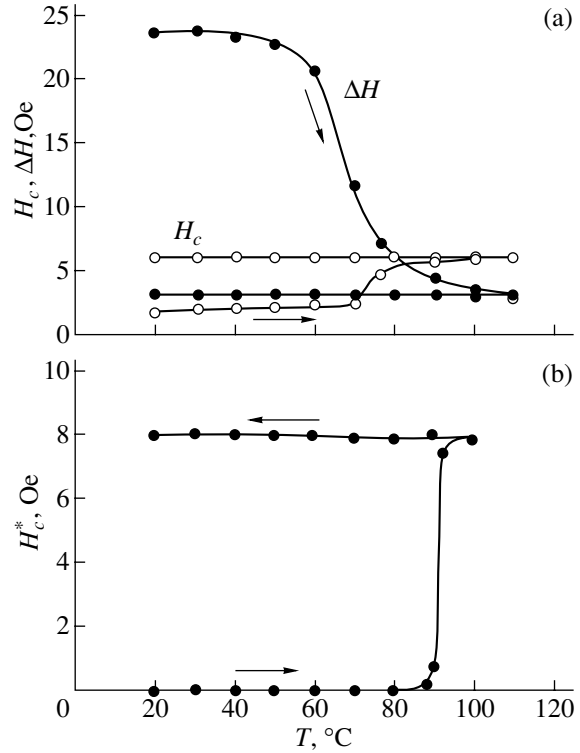


**Fig. 3.** Heating-cooling cycle of the TbFe/NiFe film system along the (a) EMA and (b) HMA.

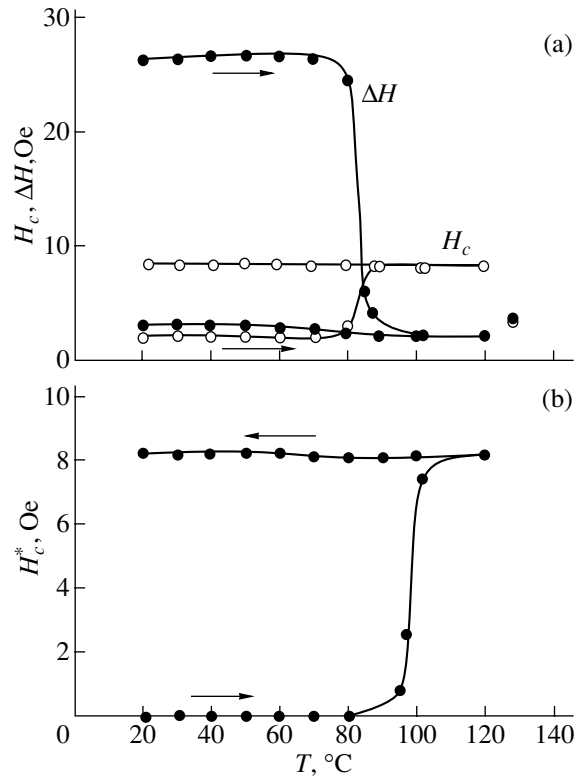


**Fig. 4.** Same as in Fig. 3 for DyCo/NiFe: (a) along the EMA and (b) along the HMA.

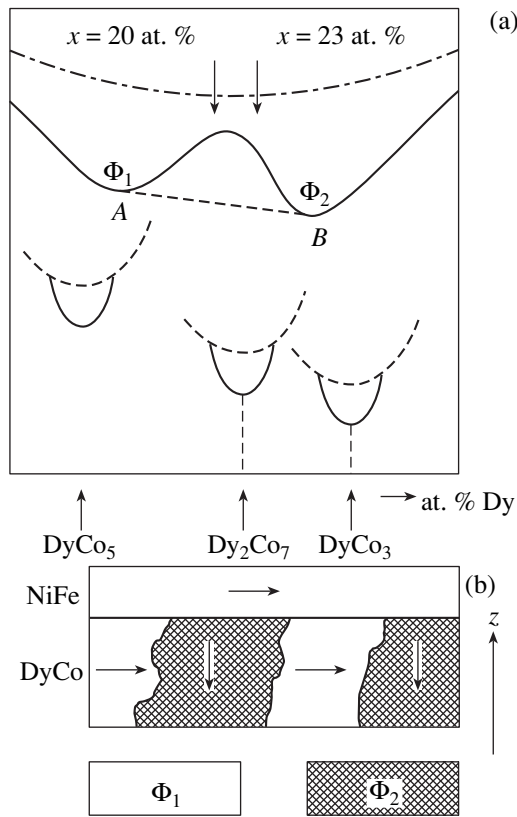


**Fig. 5.** Schematic drawings of (a) a portion of the phase diagram and (b) the hypothetical configuration of the magnetization vectors of the phases in the DyCo/NiFe system.

same transition in DyCo/NiFe is observed at a higher temperature ( $\sim 100^\circ\text{C}$ ).

#### 4. DISCUSSION

The  $\text{Dy}_{22}\text{Co}_{78}/\text{Ni}_{81}\text{Fe}_{19}$  bilayer films produced are exchange-biased systems. The hysteresis loops measured for the NiFe layer in the EMA direction are characterized by the bias field  $\Delta H$ , whose numerical values depend on the thicknesses of individual layers (table). At the same time, the significant perpendicular magnetic anisotropy in the DyCo magnetically hard ferrimagnetic layer, as well as the identical magneto-optical characteristics measured at different surfaces of the DyCo uniaxial film, indicate the following circumstance. In order to induce the required exchange field in the NiFe ferromagnetic film, the DyCo layer must contain percolation regions that emerge to its outer surfaces. In these regions, the magnetization vector of the sublattice of Co atoms should be aligned with the film plane. In our opinion, the exchange interaction of these regions with permalloy causes unidirectional exchange anisotropy. Thus, the static magnetic characteristics of the NiFe alloy layer can serve as an indicator of the magnetic microstructure of the DyCo alloy layer.

We believe that the magnetic inhomogeneity of DyCo (the regions comprising the major portion of the alloy in which the magnetization vector of the sublattice of Co atoms is perpendicular to the film plane and the regions in which the magnetization vector of the sublattice of Co atoms is parallel to the film plane) is associated with the heterophase composition of these alloys. Indeed, according to the results of electron microscopy (micrographs), the DyCo thin films [7, 8] are either amorphous or nanocrystalline heterophase alloys. To answer the question what is the local phase composition of the heterophase DyCo alloy films under study, one should consider a thermodynamically stable phase diagram of the DyCo crystalline alloys. We note that the melting diagrams of the  $RE-TM$  (Ho, Tb, Dy, Er, Gd, etc.)-(Fe, Co) alloys are similar to one another and that they present a number of stoichiometric compounds:  $RE_2TM_{17}$ ,  $RETM_5$ ,  $RE_2TM_7$ ,  $RETM_3$ ,  $RETM_2$ , and  $RE_4TM_3$  [12]. The only difference lies in the temperature range of stability of these stoichiometric compounds.

Figure 5a shows a schematic drawing of the portion of the room-temperature phase diagram on the coordinates  $(G, C)$ , where  $G$  is the Gibbs thermodynamic potential and  $C$  is the concentration in the range of compositions close to that of the films studied. Thermodynamic potentials  $G_i$  in the form of parabolas corresponding to the stoichiometric compounds  $\text{DyCo}_5$ ,  $\text{Dy}_2\text{Co}_7$ , and  $\text{DyCo}_3$  are also shown in Fig. 5a. The Gibbs potential of the melt (liquid phase) is plotted by the dash-dotted curve. The crystalline-to-amorphous or crystalline-to-nanocrystalline phase transition is accompanied, first, by an increase in the absolute values of the potentials and, second, by broadening of the parabolas describing the potentials  $G_i$  of the individual phases. The superposition of the  $G_i$  curves for alloys in the nanocrystalline state is shown in Fig. 5a by the heavy curve. The compositions of the DyCo alloy films we studied are indicated by arrows. Line  $AB$  corresponds to the possible phase composition of the mechanical mixture of the phases  $\Phi_1$  and  $\Phi_2$ . Since the stoichiometric compounds  $\text{DyCo}_5$ ,  $\text{Dy}_2\text{Co}_7$ , and  $\text{DyCo}_3$  are characterized by similar closely packed structures [12], the crystal structures of the phases  $\Phi_1$  and  $\Phi_2$  are also similar to each other. However, in contrast to the crystal structures of the stoichiometric compounds  $\text{DyCo}_5$ ,  $\text{Dy}_2\text{Co}_7$ , and  $\text{DyCo}_3$ , their room-temperature magnetic characteristics differ significantly [12, 13]. At room temperature, the magnetization of the Co sublattice in the DyCo crystal is stronger than that of the Dy sublattice:  $M_{\text{Co}} > M_{\text{Dy}}$ . In the case of the  $\text{DyCo}_3$  crystal, the situation is reversed.

Thus, we assume that the dominant phase in the DyCo film is the  $\Phi_2$  phase with  $M_{\text{Co}} < M_{\text{Dy}}$  at room temperature. The total magnetization  $M_s$  of this phase is orthogonal to the film plane. In our opinion, it is this phase that is responsible for the integral magnetic char-

acteristics of the  $\text{Dy}_{22}\text{Co}_{78}$  alloy film. For the  $\Phi_1$  phase, which is an impurity phase, we have  $M_s = M_{\text{Co}} - M_{\text{Dy}}$ . It is probable that the short-range order of the  $\Phi_1$  phase is close to the stoichiometric compound  $\text{DyCo}_5$ . The small grain size ( $\sim 5$  nm) of the nanocrystalline heterophase alloy and the exchange interaction between the Co sublattices of the  $\Phi_1$  and  $\Phi_2$  phases cause  $M_{\text{Co}}$  of the  $\Phi_1$  phase to be parallel to the film plane. The assumed configuration of the magnetization vectors of 3d metals in the  $\text{Dy}_{22}\text{Co}_{78}/\text{Ni}_{81}\text{Fe}_{19}$  bilayer films is shown in Fig. 5b. The exchange interaction between the magnetization of the  $\text{Ni}_{81}\text{Fe}_{19}$  layer and  $M_{\text{Co}}$  of the  $\Phi_1$  phase causes the unidirectional exchange anisotropy in the  $\text{Dy}_{22}\text{Co}_{78}/\text{Ni}_{81}\text{Fe}_{19}$  bilayer films.

We now discuss the temperature dependences  $\Delta H(T)$  of the bias field. The curves  $\Delta H(T)$  shown in Fig. 4 convincingly exhibit a singularity at  $T \sim 90^\circ\text{C}$ . It is necessary to pay attention to the fact that no singularities are observed in the dependences  $\Delta H(T)$  at the compensation temperature of the  $\text{Dy}_{22}\text{Co}_{78}$  ferrimagnetic magnetically hard layer ( $T_{\text{comp}} \sim 27^\circ\text{C}$ ). This indirectly indicates once again the fact that the compensation temperature is controlled by the  $\Phi_2$  phase, whose  $M_{\text{Co}}$  is orthogonal to the film plane and, hence, does not participate in the exchange interaction with the magnetization of the permalloy layer.

The disappearance of the hysteresis loop shift for the  $\text{Ni}_{81}\text{Fe}_{19}$  layer at  $T > 90^\circ\text{C}$  indicates that the plane projection of the magnetization  $M_{\text{Co}}$  of the  $\Phi_1$  phase significantly decreases above this temperature. We reason that this is caused by the magnetic phase transition in the  $\Phi_1$  phase. In our opinion, a number of magnetic transformations are possible at this temperature: (i) the transition of the  $\Phi_1$  phase to the paramagnetic state (Curie temperature); (ii)  $T \sim 90^\circ\text{C}$  is a compensation point of the  $\Phi_1$  phase; and (iii) at  $T \sim 90^\circ\text{C}$ , an orientational phase transition takes place, at which the magnetization of the  $\Phi_1$  phase emerges from the film plane and becomes parallel to the Z axis. Similar phase transitions are characteristic of the stoichiometric  $\text{RE}_x\text{TM}_y$  compounds [14]. To identify the features of the magnetic transformation in the  $\text{Dy}_{22}\text{Co}_{78}$  alloy films at  $T \sim 90^\circ\text{C}$ , additional experimental techniques need to be invoked.

## 5. CONCLUSIONS

The static magnetic characteristics of DyCo/NiFe and TbFe/NiFe bilayer exchange-biased films characterized by unidirectional anisotropy have been studied. The NiFe layer represents a magnetically soft ferromagnetic alloy whose easy magnetization axis is in the film plane. The ferrimagnetic DyCo layer with integral perpendicular anisotropy represents a heterophase nanocrystalline system consisting of at least two phases. The magnetization vector of the 3d metal sublattice of one of the components of the heterophase ferrimagnetic alloy is parallel to the film plane. In our

opinion, the exchange interaction between the magnetization of the permalloy layer and the planar component of the magnetization vector of the heterophase magnetically hard alloy causes the unidirectional anisotropy in the films under study. The magnetic transition observed at  $T \sim 90^\circ\text{C}$  (where the unidirectional anisotropy disappears in the bilayer films under consideration) takes place in one of the components of the nanocrystalline heterophase alloy  $\text{Dy}_{22}\text{Co}_{78}$ . This magnetic transformation in the DyCo alloy films is revealed for the first time. To ascertain its character, additional methods need to be invoked.

## ACKNOWLEDGMENTS

This study was supported by the Krasnoyarsky Krai Science Foundation–Russian Foundation for Basic Research, project no. 02-02-97717.

## REFERENCES

1. W. H. Meiklejohn and C. P. Bean, *Phys. Rev.* **105** (3), 904 (1957).
2. A. A. Glazer, R. I. Tagirov, A. P. Potapov, and Ya. S. Shur, *Fiz. Tverd. Tela (Leningrad)* **8** (10), 3022 (1966) [*Sov. Phys. Solid State* **8**, 2413 (1966)].
3. A. Yelon, in *Physics of Thin Films: Advances in Research and Development*, Ed. by M. H. Francombe and R. W. Hoffman (Academic, New York, 1971; Mir, Moscow, 1973), Vol. 6.
4. V. S. Gornakov, V. I. Nikitenko, A. I. Shapiro, *et al.*, in *Proceedings of XVII International School–Seminar on New Magnetic Materials in Microelectronics* (Mosk. Gos. Univ., Moscow, 2000).
5. V. A. Seredkin, G. I. Frolov, and V. Yu. Yakovchuk, *Pis'ma Zh. Tekh. Fiz.* **9** (23), 1446 (1983) [*Sov. Tech. Phys. Lett.* **9**, 621 (1983)].
6. V. V. Polyakov, G. I. Frolov, A. G. Vladimirov, and V. Yu. Yakovchuk, in *Abstracts of VII All-Union Conference on Problems of Magnetic Measurements and Magnetic Instrumentation, Leningrad* (1990), p. 97.
7. L. I. Vershinina, N. D. Zakharov, S. Z. Sklyuev, *et al.*, *Fiz. Met. Metalloved.* **66** (2), 278 (1988).
8. E. M. Artem'ev, L. I. Vershinina, V. G. Myagkov, *et al.*, *Fiz. Met. Metalloved.*, No. 2, 77 (1990).
9. V. A. Seredkin, G. I. Frolov, and V. Yu. Yakovchuk, *Fiz. Met. Metalloved.* **63** (3), 457 (1987).
10. R. S. Iskhakov, V. Yu. Yakovchuk, S. V. Stolyar, *et al.*, *Fiz. Tverd. Tela (St. Petersburg)* **43** (8), 1462 (2001) [*Phys. Solid State* **43**, 1522 (2001)].
11. G. V. Popov, V. A. Seredkin, G. I. Frolov, and V. Yu. Yakovchuk, *Fiz. Met. Metalloved.*, No. 2, 61 (1990).
12. E. M. Savitskiĭ and V. F. Terekhova, *Physical Metallurgy of Rare-Earth Metals* (Nauka, Moscow, 1975).
13. E. V. Shcherbakova and A. S. Ermolenko, *Fiz. Met. Metalloved.* **59** (2), 344 (1985).
14. A. S. Ermolenko, E. V. Rozenfel'd, Yu. P. Irkhin, *et al.*, *Zh. Èksp. Teor. Fiz.* **69**, 1743 (1975) [*Sov. Phys. JETP* **42**, 885 (1975)].

*Translated by A. Kazantsev*